The EMBO Journal Vol. 22 No. 23 pp. 6234–6244, 2003

The phosphorylation state of an autoregulatory domain controls PACS-1-directed protein traffic

Gregory K.Scott, Feng Gu[1], Colin M.Crump[2], Laurel Thomas, Lei Wan, Yang Xiang[3] and Gary Thomas[4]

Vollum Institute, L-474, 3181 SW Sam Jackson Park Road, Portland, OR 97239, [3]Department of Molecular and Cellular Physiology, Stanford Medical Center, Palo Alto, CA 94305, USA, [1]McGill Cancer Center, McGill University, 3655, Promenade Sir William Osler, Montreal, Quebec, H3G 1Y6, Canada and [2]Division of Virology, Department of Pathology, University of Cambridge, Tennis Court Road, Cambridge CB2 1QP, UK

[4]Corresponding author
e-mail: thomasg@ohsu.edu

G.K.Scott and F.Gu contributed equally to this work

PACS-1 is a cytosolic sorting protein that directs the localization of membrane proteins in the *trans*-Golgi network (TGN)/endosomal system. PACS-1 connects the clathrin adaptor AP-1 to acidic cluster sorting motifs contained in the cytoplasmic domain of cargo proteins such as furin, the cation-independent mannose-6-phosphate receptor and in viral proteins such as human immunodeficiency virus type 1 Nef. Here we show that an acidic cluster on PACS-1, which is highly similar to acidic cluster sorting motifs on cargo molecules, acts as an autoregulatory domain that controls PACS-1-directed sorting. Biochemical studies show that Ser278 adjacent to the acidic cluster is phosphorylated by CK2 and dephosphorylated by PP2A. Phosphorylation of Ser278 by CK2 or a Ser278→Asp mutation increased the interaction between PACS-1 and cargo, whereas a Ser278→Ala substitution decreased this interaction. Moreover, the Ser278→Ala mutation yields a dominant-negative PACS-1 molecule that selectively blocks retrieval of PACS-1-regulated cargo molecules to the TGN. These results suggest that coordinated signaling events regulate transport within the TGN/endosomal system through the phosphorylation state of both cargo and the sorting machinery.

Keywords: autoregulatory domain/CK2/Nef/PACS-1/phosphorylation

Introduction

The control of homeostasis and disease requires that cellular or pathogen proteins are correctly modified and targeted to specific cellular compartments. Many of these modification and targeting steps rely on the communication between the dynamic and highly regulated network of late secretory pathway organelles that comprise the *trans*-Golgi network (TGN)/endosomal system (Gruenberg, 2001). In addition to housing several biochemical reactions, the TGN orchestrates the routing of proteins to lysosomes, secretory granules and, in polarized cells, the apical and basolateral surfaces. The TGN also receives molecules internalized from the cell surface via a series of complex and highly dynamic endosomal compartments. Precisely how the TGN/endosomal system controls the sorting and localization of proteins is incompletely understood, but numerous studies show the requirement for the orchestrated interaction of many cellular factors including various small molecules, lipids, cytosolic and membrane proteins and components of the cytoskeleton (Gu *et al*., 2001).

The localization of many membrane proteins within the TGN/endosomal system relies upon specific sorting motifs contained within the cytoplasmic domain of these proteins (Bonifacino and Traub, 2003). One of these motifs is represented by clusters of acidic residues, often containing serine or threonine residues that can be phosphorylated by casein kinase 2 (CK2) or, less frequently, casein kinase 1 (CK1) (for reviews see Gu *et al*., 2001; Thomas, 2002; Bonifacino and Traub, 2003). Membrane proteins that contain acidic sorting motifs include processing enzymes such as furin (Jones *et al*., 1995), PC6B (Xiang *et al*., 2000) and carboxypeptidase D (CPD; Kalinina *et al*., 2002); receptors such as the cation-independent mannose-6-phosphate receptor (CI-MPR; Chen *et al*., 1997); transporters such as VMAT2 (Waites *et al*., 2001); SNAREs including VAMP-4 (Zeng *et al*., 2003); and a number of pathogenic molecules including the envelope glycoproteins of many herpesviruses such as varicella-zoster virus gE (VZV-gE; Alconada *et al*., 1999) and human cytomegalovirus gB (HCMV-gB; Norais *et al*., 1996), as well as human immunodeficiency virus type 1 (HIV-1) Nef (Piguet *et al*., 2000). Perhaps the best studied of these acidic cluster motifs is the one present in the cytoplasmic domain of furin (Thomas, 2002). The phosphorylation state of the furin acidic cluster controls in large part the dynamic sorting itinerary of the endoprotease including the localization of furin to the TGN (Jones *et al*., 1995), recycling of furin from early endosomes to the cell surface (Molloy *et al*., 1998) and, in neuroendocrine cells, removal of furin from immature secretory granules (Dittie *et al*., 1997). In contrast, dephosphorylation of the furin acidic cluster by specific isoforms of protein phosphatase 2A (PP2A) allows transport of furin between endosomal compartments (Molloy *et al*., 1998). Thus, the coordinated activities of CK2 and PP2A control the complex, acidic cluster-mediated trafficking of furin.

The phosphorylated furin acidic cluster binds to the sorting protein PACS-1 (phosphofurin acidic cluster sorting protein-1), which is a sorting connector that links furin to the AP-1 clathrin adaptor and is required for localizing furin to the TGN (Wan *et al*., 1998; Crump *et al*., 2001). PACS-1 is not dedicated exclusively to the localization of furin, as it is also required for the TGN

© European Molecular Biology Organization

localization of a number of membrane proteins that contain acidic cluster sorting motifs. These include cellular proteins, such as CI-MPR (Wan *et al*., 1998), PC6B (Xiang *et al*., 2000) and VMAT2 (Waites *et al*., 2001), as well as several viral proteins including HCMV-gB (Crump *et al*., 2003) and HIV-1 Nef (Piguet *et al*., 2000). PACS-1 binding to HIV-1 Nef is required for the ability of this viral protein to downregulate cell surface major histocompatibility class-I (MHC-I) complexes (Piguet *et al*., 2000; Blagoveshchenskaya *et al*., 2002).

While the importance of PACS-1 for localizing acidic cluster-containing membrane cargo to the TGN is well established, no information pertaining to the regulation of its sorting activity has been reported. For many cargo molecules including furin, CI-MPR, VMAT2 and VZV-gE, phosphorylation of specific residues within their acidic clusters enhances binding to PACS-1 (Wan *et al*., 1998; Waites *et al*., 2001), whereas others including PC6B and HIV-1 Nef contain non-phosphorylatable acidic clusters (Piguet *et al*., 2000; Xiang *et al*., 2000). Together, these results suggest that binding of PACS-1 to cargo acidic clusters may be regulated by more than just the phosphorylation state of the cargo protein. Interestingly, PACS-1 itself contains an acidic cluster with a potential CK2 phosphorylation site, -S_{278}EEEEE-, located C-terminal to the cargo-binding domain (named the FBR, see Figure 1A). The striking similarity between the acidic clusters in PACS-1 and those in cargo molecules such as furin raises the possibility that the PACS-1 acidic cluster may control PACS-1 sorting activity.

In this report, we show that the PACS-1 acidic cluster acts as an autoregulatory domain for PACS-1-directed protein trafficking and is itself a target of CK2 phosphorylation and PP2A dephosphorylation. We demonstrate that the PACS-1 acidic cluster associates with the cargo-binding region of PACS-1 in a phosphorylation-dependent manner. Using biochemical, cellular and cell-free studies, we show that the phosphorylation state of the PACS-1 acidic cluster regulates the ability of PACS-1 to bind to and sort cargo proteins to the TGN. Disruption of PACS-1 phosphorylation by a Ser278→Ala substitution results in an interfering mutant that inhibits PACS-1-directed endosome to TGN sorting. These results provide new insight into how a coordinated signaling mechanism controlling the phosphorylation of both the cargo and a sorting connector can regulate TGN/endosomal sorting.

Results

Inspection of the PACS-1 protein sequence reveals an acidic cluster, -S_{278}EEEEE-, C-terminal to the cargo-binding region (FBR, residues 117–266) that is similar to the acidic cluster sorting motifs on many membrane cargo proteins that bind to the PACS-1 FBR (Figure 1A). Interestingly, the serine residue within the PACS-1 acidic cluster forms a consensus sequence for CK2 phosphorylation. To determine if Ser278 is a major site of phosphorylation in PACS-1, cells expressing wild-type PACS-1 or PACS-1 with a Ser278→Ala substitution (PACS-1S_{278}A) were incubated with $^{32}P_i$ and the immunoprecipitated PACS-1 proteins were resolved by SDS–PAGE. Quantification of the incorporated radioactivity showed that PACS-1S_{278}A contained 50% less ^{32}P than wild-type PACS-1, indicating that Ser278 is a major PACS-1 phosphorylation site *in vivo* (Figure 1B).

Next we conducted a series of *in vitro* studies to characterize the reversible phosphorylation of PACS-1 at Ser278. First, we showed that Ser278 could be phosphorylated by CK2 (Figure 1C). GST–PACS-$1_{240–479}$ (GST–MR, which contains the PACS-1 acidic cluster) or GST–MRS_{278}A was incubated with purified CK2 and [γ-^{32}P]ATP. GST–MRS_{278}A incorporated significantly less ^{32}P than did GST–MR, suggesting that Ser278 within the PACS-1 acidic cluster is a substrate for CK2. Moreover, neither protein kinase A nor protein kinase C could phosphorylate GST–MR despite their ability to phosphorylate a control substrate efficiently (data not shown). Secondly, to identify Ser278 unequivocally as a CK2 phosphorylation site, we conducted phosphoamino acid analysis on GST–MRS_{278}T following CK2 phosphorylation (Figure 1D). The Ser278→Thr substitution was chosen because GST–MR lacks a phosphorylatable threonine residue. Thus, the formation of pThr in GST–MRS_{278}T following incubation with CK2 must be due to phosphorylation at residue 278. Replicate samples of GST–MR, GST–MRS_{278}A and GST–MRS_{278}T were incubated with recombinant CK2 and [γ-^{32}P]ATP. Phosphoamino acid analysis of GST–MR and GST–MRS_{278}A showed a prominent signal of only pSer. In contrast, analysis of GST–MRS_{278}T revealed pThr in addition to pSer. These data strongly indicate that Ser278 is a major CK2 phosphorylation site in PACS-1. Thirdly, because many cargo acidic cluster motifs that require CK2 phosphorylation for binding to PACS-1 are dephosphorylated by PP2A (Molloy *et al*., 1998; Varlamov *et al*., 2001), we investigated whether PP2A can similarly dephosphorylate the CK2-phophorylated GST–MR (Figure 1E). Consistent with a potential role for PP2A at this step, [^{32}P]GST–MR was dephosphorylated efficiently by PP2A and this reaction was blocked by okadaic acid (OA), a PP2A-specific inhibitor. In contrast, protein phosphatase 1 (PP1) failed to dephosphorylate [^{32}P]GST–MR despite its ability to dephosphorylate a control substrate efficiently (data not shown), suggesting a role for PP2A as the PACS-1 Ser278 phosphatase.

We conducted metabolic labeling studies to determine whether endogenous PACS-1 is phosphorylated *in vivo*. Cells were incubated with $^{32}P_i$ and endogenous PACS-1 was immunoprecipitated with affinity-purified anti-PACS-1 antibodies but not with an IgG control (Figure 1F). In agreement with our *in vitro* studies, incubation of the cells with OA increased the amount of ^{32}P incorporated into PACS-1 by 2-fold. In contrast, and in agreement with the analysis of PACS-1S_{278}A (Figure 1B), incubation of the cells with the CK2 inhibitor 5,6-dichlorobenzimidazole riboside (DRB) decreased the amount of ^{32}P incorporated into endogenous PACS-1 by ~50% relative to control conditions. Together with our *in vitro* studies, these data strongly implicate CK2 and PP2A as the enzymes that control the phosphorylation state of PACS-1 Ser278.

The reversible phosphorylation of Ser278 raised the possibility that, similarly to PACS-1 cargo proteins, the PACS-1 acidic cluster may interact with the PACS-1 FBR. To test this possibility, non-phosphorylated or CK2-phosphorylated GST–MR was incubated with thioredoxin (Trx)–PACS-1 FBR and captured using glutathione–

agarose (Figure 2A). We found that GST–PACS-1 MR indeed bound to Trx–PACS-1 FBR. Surprisingly, however, whereas phosphorylation of most PACS-1 cargo proteins enhanced binding to the PACS-1 FBR, the phosphorylation of GST–PACS-1 MR by CK2 diminished binding to Trx–PACS-1 FBR. To test whether this reduced binding was due specifically to phosphorylation of Ser278, we measured the binding of the PACS-1 FBR to GST–MR constructs containing either a Ser278→Ala or a Ser278→Asp substitution. Consistent with the results

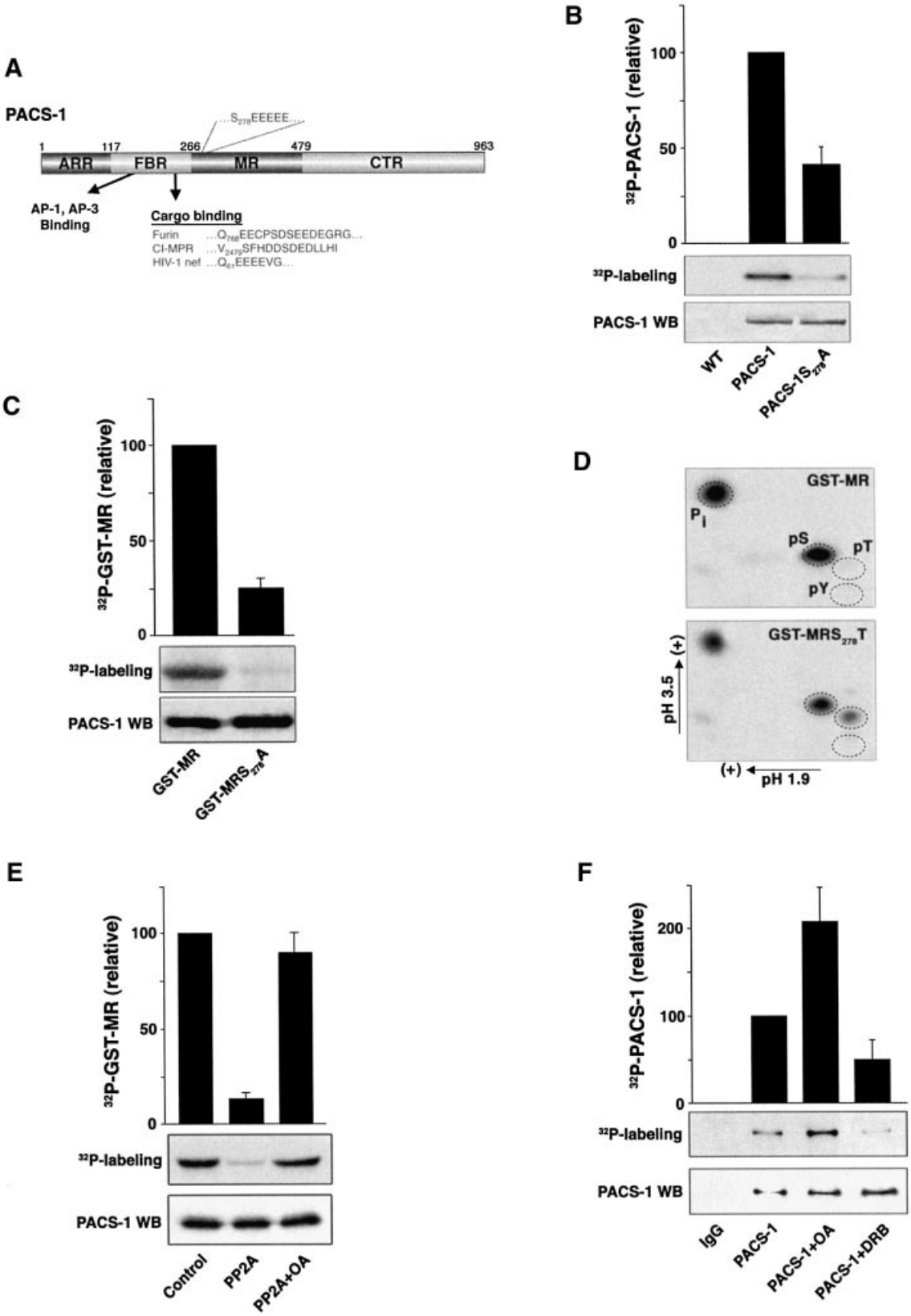

using CK2-phosphorylated molecules, GST–MRS_{278}A exhibited stronger binding to Trx–PACS-1 FBR than the GST–MRS_{278}D.

We performed competitive binding assays to test whether GST–MR, which contains the PACS-1 acidic cluster, competes with cargo protein acidic clusters for binding to the PACS-1 FBR (Figure 2B). GST–PACS-1 MR was pre-incubated with Trx–PACS-1 FBR and then mixed with increasing concentrations of either Trx or Trx–furin$S_{773,775}$D, which contains the CK2 phosphomimic furin cytoplasmic domain that binds to the PACS-1 FBR (Wan *et al*., 1998). GST–PACS-1 MR was captured using glutathione–agarose, and bound Trx–PACS-1 FBR was detected by western blot. Using this assay, we found that Trx–furin$S_{773,775}$D competed in a dose-dependent manner with GST–MR for binding to the PACS-1 FBR, whereas Trx alone had no effect. Together, the data in Figure 2A and B indicate that binding of the PACS-1 MR to the PACS-1 FBR precludes cargo binding to PACS-1.

To examine the importance of Ser278 phosphorylation in the context of full-length PACS-1, we tested the ability of PACS-1S_{278}A or PACS-1S_{278}D to bind to the PACS-1 cargo protein HIV-1 Nef (Figure 2C). We previously showed that the Nef acidic cluster, $EEEE_{65}$, is required for binding to PACS-1 and for PACS-1-dependent sorting of HIV-1 Nef reporter proteins to the TGN (Piguet *et al*., 2000; Blagoveshchenskaya *et al*., 2002). Because the Nef acidic cluster cannot be phosphorylated by CK2, only CK2 phosphorylation of the putative PACS-1 autoregulatory domain may regulate Nef–PACS-1 binding. Cells expressing PACS-1, PACS-1S_{278}A or PACS-1S_{278}D were harvested and incubated with GST–Nef. Quantification of proteins binding to HIV-1 Nef showed that the S_{278}D substitution enhanced PACS-1 binding to GST–Nef by >50%, whereas the S_{278}A substitution inhibited PACS-1 binding to GST–Nef by nearly 80%. Thus, the ability of PACS-1 to bind cargo is regulated by the phosphorylation state of Ser278.

The Ser278→Ala/Asp substitutions could potentially inhibit the interaction of PACS-1 with adaptor complexes due to some indirect structural deformation. To test this possibility, PACS-1 proteins were immunoprecipitated from cells expressing PACS-1, PACS-1S_{278}A, PACS-1S_{278}D or PACS-1Admut, which contains an alanine substitution of E_{168}TELQLTF_{175} within the PACS-1 FBR that blocks binding to adaptor complexes but not cargo (Crump *et al*., 2001). Co-immunoprecipitation analysis showed that each PACS-1 construct, except PACS-1Admut, associated with AP-1 (Figure 2D). Together, the data in Figure 2 show that phosphorylation at Ser278 terminates the autoinhibitory domain to the cargo-binding domain, thereby promoting binding of PACS-1 to cargo proteins.

The inhibitory effect of the Ser278→Ala substitution on the ability of PACS-1 to bind cargo proteins suggested that expression of PACS-1S_{278}A in cells might interfere with PACS-1-dependent sorting. Therefore, we examined the effect of PACS-1S_{278}A and PACS-1S_{278}D on the TGN sorting of the HIV-1 Nef reporter construct 44Nef (Figure 3A). 44Nef is a chimera composed of the CD4 extracellular and transmembrane domains fused to cytoplasmic HIV-1 Nef. Using this construct, CD4 antibody uptake assays showed that co-expression of the reporter with either PACS-1 or PACS-1S_{278}D had no effect on the efficient delivery of internalized 44Nef to the TGN. In contrast, co-expression of PACS-1S_{278}A blocked the sorting of internalized 44Nef to the TGN and caused the reporter to be mislocalized to a dispersed, punctate endosomal population. The interfering effect of PACS-1S_{278}A on the sorting of 44Nef to the TGN was indistinguishable from the missorting of 44NefAla, which contains an $EEEE_{65}$→$AAAA_{65}$ substitution that cannot bind to PACS-1 (Piguet *et al*., 2000).

Next, we used a cell-free assay to establish unequivocally the role of PACS-1, and in particular the phosphorylation state of Ser278, in endosome to TGN sorting (Figure 3B). This assay utilizes the activity of a TGN resident tyrosylprotein sulfotransferase that sulfates tyrosine residues in the lumenal domain of cargo proteins to demonstrate sorting to the TGN. A 44Nef mutant, 44Nef-Y, was constructed containing the cholecystokinin tyrosine O-sulfation motif within the CD4 lumenal domain. Cells expressing 44Nef-Y were treated with cycloheximide to block protein synthesis and promote accumulation of the nascently synthesized 44Nef-Y in late secretory pathway compartments. The membrane fraction from these cells was incubated with the unlabeled sulfate donor PAPS (3′-phosphoadenosine 5′-phosphosulfate) to quench any 44Nef-Y present at the TGN but not in endosomal compartments, which lack the sulfotransferase. The quenched membrane preparation was then incubated with cytosol from control C6 cells, AS19 PACS-1

Fig. 1. PACS-1 Ser278 is phosphorylated by CK2 and dephosphorylated by PP2A. (**A**) Schematic diagram of PACS-1 showing the atrophin-related region (ARR), the furin-binding region (FBR) which interacts with cargo molecules and AP-1/AP-3 adaptor complexes, the middle region (MR) which contains the autoregulatory acidic cluster and Ser278, and the C-terminal region (CTR). The acidic cluster in the PACS-1 MR as well as acidic cluster sequences contained in membrane cargo molecules, which bind to the PACS-1 FBR, are indicated. (**B**) *In vivo* phosphorylation of expressed PACS-1. BSC40 cells infected with VV recombinants expressing either epitope (HA)-tagged PACS-1 or PACS-1S_{278}A were labeled with $^{32}P_i$, and the immunoprecipitated PACS-1 proteins were separated by SDS–PAGE and analyzed by autoradiography (upper panel). A western blot using the anti-HA mAb HA.11 shows equal expression and loading of the two proteins (lower panel). (**C**) *In vitro* CK2 phosphorylation of GST–MR. GST–MR or GST–MRS_{278}A was incubated with CK2 and [γ-^{32}P]ATP, separated by SDS–PAGE and analyzed by autoradiography. (**D**) PACS-1 MR is phosphorylated at amino acid 278. GST–MR or GST–MRS_{278}T was phosphorylated by CK2 with [γ-^{32}P]ATP, separated by SDS–PAGE, transferred to PVDF, acid hydrolyzed, and subjected to two-dimensional thin-layer chromatography. The positions of phosphoserine (pS), phosphothreonine (pT) and phosphotyrosine (pY) standards are shown. (**E**) PP2A dephosphorylates GST–PACS-1 MR. *In vitro* CK2-phosphorylated [^{32}P]GST–MR was incubated without (control) or with recombinant PP2A in the presence or absence of 10 nM OA, separated by SDS–PAGE and analyzed by autoradiography. (**F**) CK2 and PP2A regulate phosphorylation of endogenous PACS-1 *in vivo*. A7 cells were labeled with $^{32}P_i$, treated or not with either 100μM DRB or 20 nM OA, and endogenous PACS-1 was immunoprecipitated, separated by SDS–PAGE and analyzed by autoradiography. All autoradiography was quantified using NIH image 1.61 software. ^{32}P incorporation was normalized to PACS-1 protein loading and is presented relative to control PACS-1 phosphorylation. Bar graphs represent the mean ± SE of at least three separate experiments.

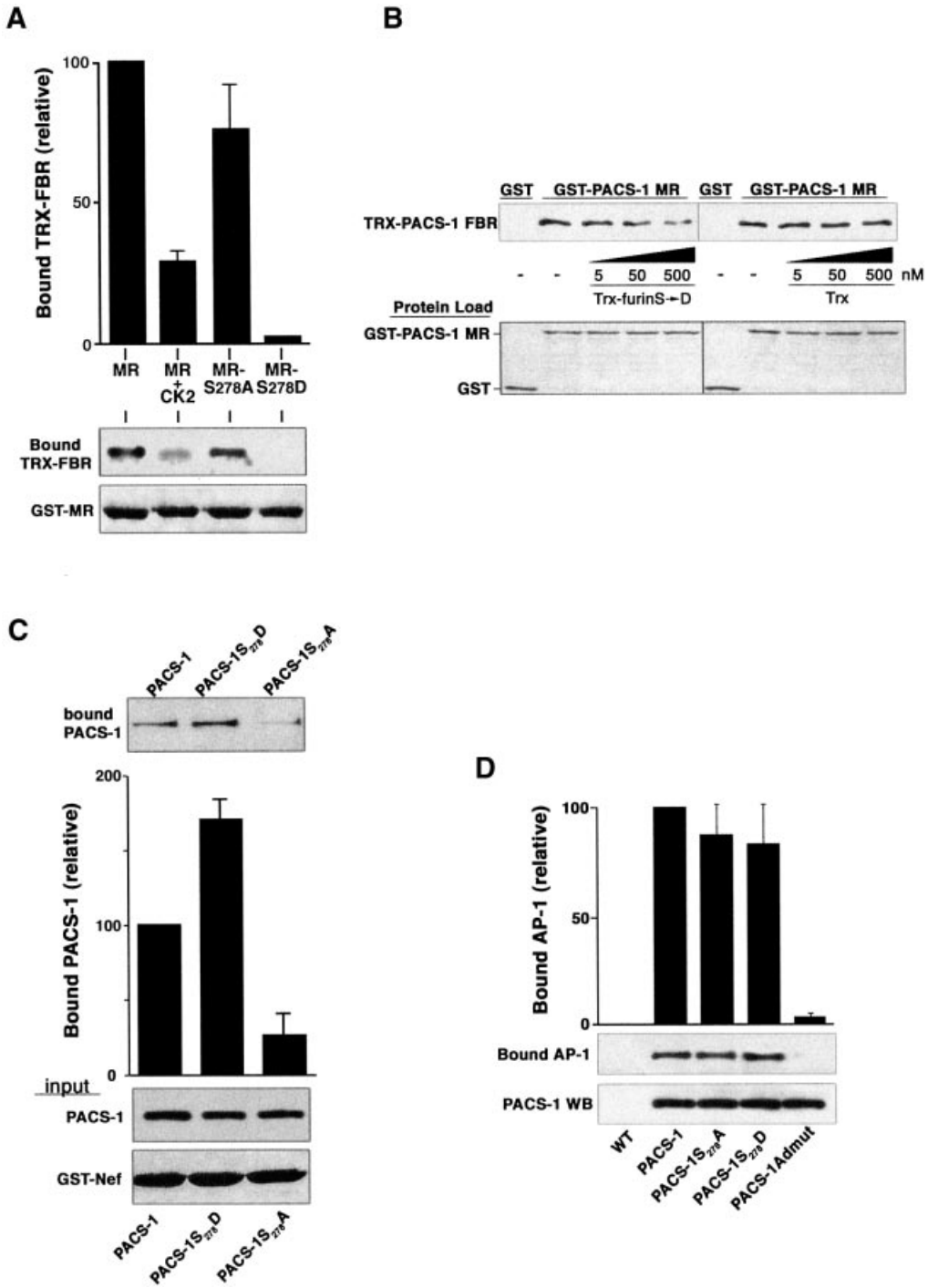

Fig. 2. Phosphorylation of PACS-1 Ser278 promotes PACS-1 binding to cargo proteins. (**A**) Phosphorylation of PACS-1 Ser278 inhibits PACS-1 MR binding to the PACS-1 FBR. GST–MR, GST–MRS_{278}A, GST–MRS_{278}D or CK2-phosphorylated GST–MR were incubated with Trx–PACS-1 FBR and captured using glutathione–agarose. Bound Trx–PACS-1 FBR was analyzed by western blot (upper panel). Incomplete phosphorylation of GST–MR may explain the slightly greater binding of Trx–PACS-1 FBR to CK2-phosphorylated GST–MR compared with GST–MRS_{278}D. (**B**) The PACS-1 MR acidic cluster competes with cargo proteins for binding to the PACS-1 FBR. GST capture assays were performed as in (A), with the addition of varying concentrations of Trx–furin$S_{773,775}$D (Trx-furin S→D) or Trx alone to the binding reaction. (**C**) Ser278 regulates binding to cargo proteins. Epitope-(HA)-tagged PACS-1, PACS-1S_{278}A and PACS-1S_{278}D were expressed in replicate plates of A7 cells using VV recombinants. Cell lysates were incubated with GST–Nef, and GST–Nef was captured using glutathione–agarose. PACS-1 proteins bound to GST–Nef were analyzed by western blot using the anti-HA mAb HA.11 (top panel). GST–Nef input and expression of PACS-1 proteins is shown (lower panels). (**D**) Mutation of PACS-1 Ser278 does not affect binding to AP-1. Epitope-(HA)-tagged PACS-1, PACS-1S_{278}A, PACS-1S_{278}D or PACS-1Admut were expressed in A7 cells and immunoprecipitated with mAb HA.11. Precipitated proteins were separated by SDS–PAGE and analyzed by western blot using mAb 100/3 (AP-1) or mAb PACS-1. All data were quantified as described in the legend to Figure 1.

antisense cells or AS19 cells expressing PACS-1, PACS-1S_{278}D or PACS-1S_{278}A. Each sample was incubated with an ATP-regenerating system in the presence of [^{35}S]PAPS to promote endosome to TGN transport. Using this assay, we found that addition of cytosol from control cells (C6) but not cytosol from PACS-1 antisense cells (AS19),

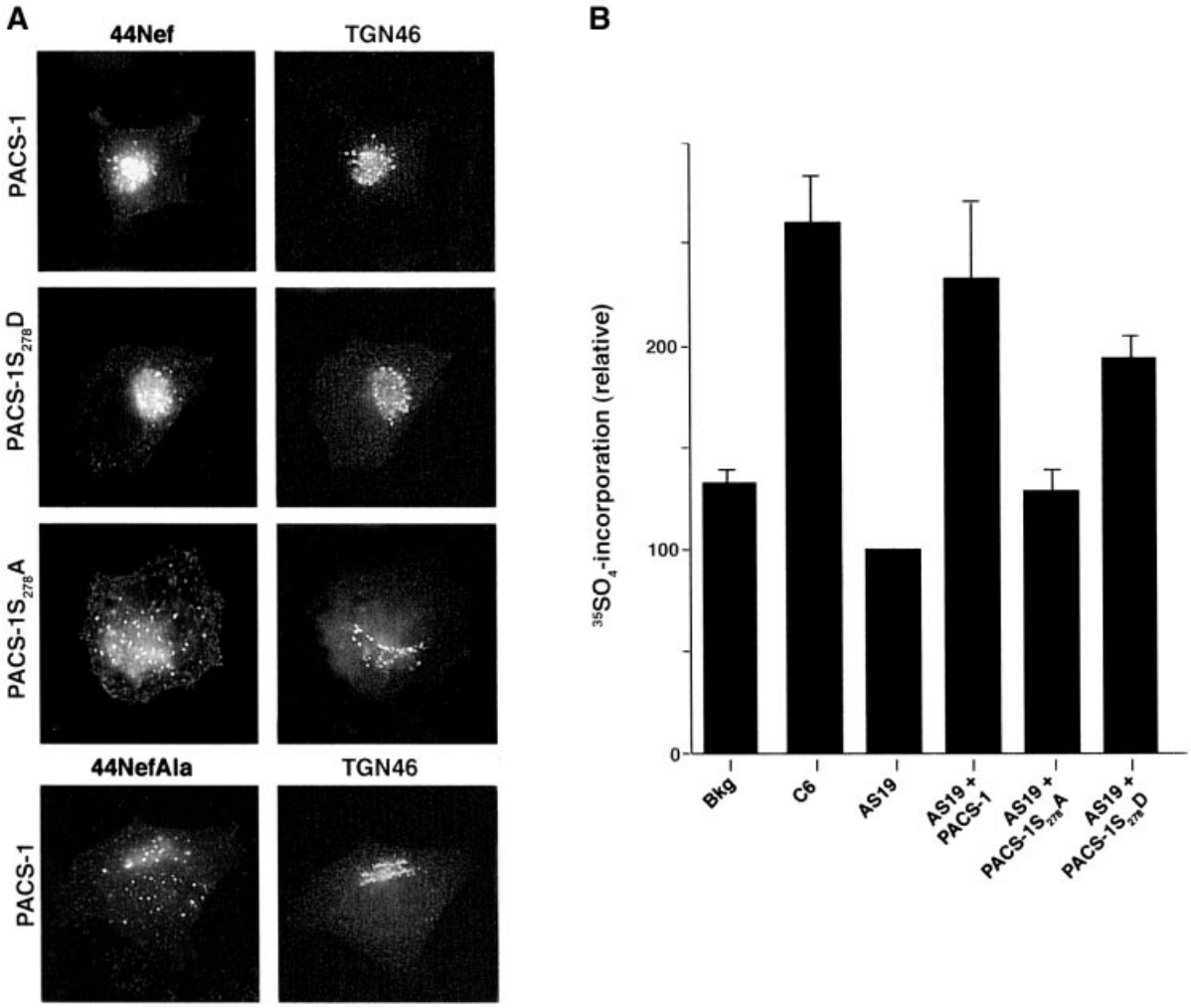

Fig. 3. Phosphorylated PACS-1 directs endosome to TGN transport. (**A**) PACS-1S_{278}A expression disrupts the TGN localization of 44Nef. A7 cells were infected with recombinant virus expressing 44Nef as well as PACS-1, PACS-1S_{278}A or PACS-1S_{278}D. Localization of 44Nef was determined by CD4 antibody uptake. The cells were fixed, permeabilized and co-stained with the TGN marker anti-TGN46 followed by fluorescent secondary antisera. As a control, a mutant Nef reporter, 44NefAla, which does not bind PACS-1, was also expressed. (**B**) PACS-1 directs endosome to TGN sorting in a cell-free assay. A7 cells were infected with AV expressing 44Nef-Y, after which membranes from these cells were harvested and quenched with cold PAPS. The quenched membranes were incubated in the absence (background, bkg) or presence of cytosol from C6 (control), AS19 (PACS-1 antisense) or from AS19 cells expressing PACS-1 (AS19 + PACS-1), PACS-1S_{278}A (AS19 + S_{278}A) or PACS-1S_{278}D (AS19 + S_{278}D) and with the sulfate donor [^{35}S]PAPS. 44Nef-Y was immunoprecipitated and ^{35}S incorporation was determined by autoradiography, and protein load by western blot. ^{35}S incorporation was quantified using NIH image 1.61 software, normalized for protein load and presented relative to 44Nef-Y labeling with AS19 cytosol. The bar graph represents the mean ± SE of three separate experiments.

which contain reduced levels of PACS-1, supported endosome to TGN transport as measured by an increase in ^{35}S-labeled 44Nef-Y. In contrast, cytosol from AS19 cells replete with PACS-1 rescued the endosome to TGN transport of 44Nef-Y, demonstrating the importance of PACS-1 in the retrieval of membrane cargo from endosomes to the TGN. Next, we analyzed the PACS-1 phosphorylation state of mutants and found that only PACS-1S_{278}D but not PACS-1S_{278}A rescued the endosome to TGN sorting of 44Nef-Y, supporting a role for the phosphorylation of Ser278 as a key regulator of PACS-1 sorting activity. We suspect that the less efficient rescue of 44Nef-Y sorting by PACS-1S_{278}D compared with PACS-1 may reflect a requirement for the temporal regulation of PACS-1 phosphorylation in directing protein sorting. Nonetheless, these results demonstrate that PACS-1 directs the endosome to TGN transport and that its sorting activity is regulated by the phosphorylation state of Ser278.

The immunofluorescence and *in vitro* transport studies showed that phosphorylation of PACS-1 controls the endosome to TGN transport of the 44Nef reporter and suggested that PACS-1S_{278}A may act as an interfering mutant to block the sorting of PACS-1 cargo proteins selectively. To test this possibility, we first examined the effect of PACS-1S_{278}D and PACS-1S_{278}A on the ability of HIV-1 Nef to downregulate MHC-I molecules (Figure 4). Cells expressing HIV-1 Nef alone or together with either PACS-1 or PACS-1S_{278}D caused the redistribution of cell surface MHC-I to the TGN, whereas co-expression of PACS-1S_{278}A blocked MHC-I downregulation. Secondly, we determined whether PACS-1S_{278}A could affect the TGN localization of CI-MPR and furin (Figure 5A). Expression of PACS-1 or PACS-1S_{278}D in A7 cells had no

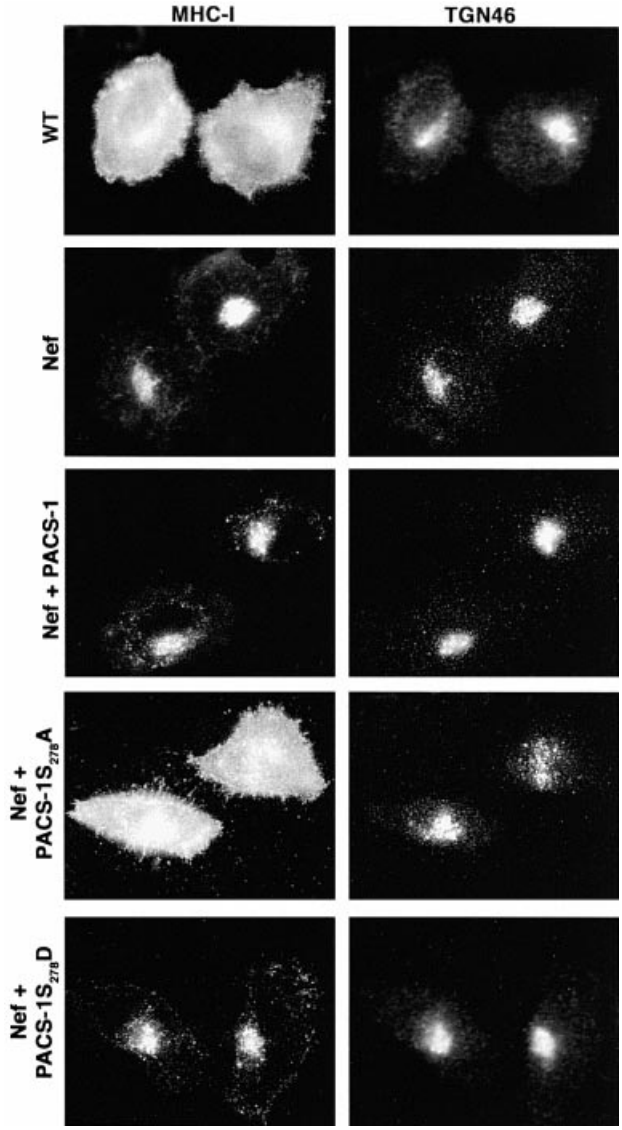

Fig. 4. Expression of PACS-1S_{278}A blocks HIV-1 Nef-mediated MHC-1 downregulation. A7 cells were infected with VV:WT or co-infected with VV recombinants expressing Nef and either PACS-1, PACS-1S_{278}A or PACS-1S_{278}D. Cells were fixed, permeabilized and incubated with anti-MHC-I and anti-TGN46 followed by fluorescently labeled secondary antisera. The expression of PACS-1 alone has no effect on MHC-I localization (Blagoveshchenskaya *et al*., 2002; and data not shown).

effect on the paranuclear localization of either endogenous CI-MPR or co-expressed Flag-tagged furin (fur/f), both of which overlapped with the staining pattern of TGN46. In contrast, expression of PACS-1S_{278}A caused both CI-MPR and fur/f to redistribute to an endosomal population that no longer overlapped with TGN46. Finally, to establish that PACS-1S_{278}A selectively blocked the sorting of PACS-1 cargo, we examined the effects of PACS-1S_{278}A and PACS-1S_{278}D on the distribution of several secretory compartment markers (Figure 5B). In addition to their lack of effect on the localization of TGN46, which does not require PACS-1 to localize to the TGN, we found that neither PACS-1 mutant affected the localization of AP-1 or markers for early endosomes (internalized transferrin), late endosomes (LBPA) or the Golgi cisternae (mannosidase II). Together, these analyses show that the sorting activity of PACS-1 is controlled by the phosphorylation state of an autoregulatory domain and that interference with this autoregulatory mechanism specifically blocks PACS-1-directed protein traffic in the TGN/endosomal system.

Discussion

In this study, we have identified a biochemical mechanism that controls the sorting activity of PACS-1. We discovered that the phosphorylation state of an autoregulatory domain within PACS-1 controls binding of this sorting connector to cargo proteins. CK2 phosphorylation of Ser278 within this autoregulatory domain weakens the interaction between the PACS-1 FBR and the PACS-1 autoregulatory domain (Figures 1 and 2), thereby enhancing binding to cargo (Figure 2). These interactions are competitive, such that the unphosphorylated PACS-1 autoregulatory domain precludes binding of cargo proteins to the PACS-1 FBR (Figure 2). Moreover, immunofluorescence and cell-free transport studies showed that both PACS-1 and the phosphomimic PACS-1 mutant, PACS-1S_{278}D, support endosome to TGN sorting of cargo (Figure 3). In contrast, the non-phosphorylatable PACS-1 mutant, PACS-1S_{278}A, fails to support this sorting step and in cellular studies disrupts both the TGN localization of PACS-1 cargo and Nef-mediated downregulation of MHC-I (Figures 4 and 5). Together, our results demonstrate that the sorting capacity of PACS-1 is regulated by the phosphorylation state of an autoregulatory domain, revealing a fundamental mechanism used to control the regulation of protein traffic in the TGN/endosomal system (Figure 6).

The control of PACS-1 function by the coordinated activities of CK2 and PP2A is highly reminiscent of the role of these two enzymes in controlling the trafficking of furin. The phosphorylation state of furin's cytoplasmic acidic cluster sorting motif, which mediates binding to PACS-1, controls the trafficking itinerary of the endoprotease (Molloy *et al*., 1999; Thomas, 2002). However, whereas CK2 phosphorylation of acidic cluster sorting motifs within the furin cytoplasmic domain or other cargo proteins including CI-MPR, VZV-gE and VMAT-2 increases their binding to the PACS-1 FBR, CK2 phosphorylation of Ser278 within the PACS-1 acidic cluster weakens the binding of these residues to the PACS-1 FBR (Wan *et al*., 1998; Waites *et al*., 2001; and Figure 2). These opposite effects of CK2 phosphorylation on binding of the PACS-1 FBR to the PACS-1 autoregulatory domain versus membrane cargo acidic clusters suggests a simple model whereby CK2 phosphorylation promotes protein sorting by both activating PACS-1 and increasing the affinity of PACS-1 for phosphorylated membrane cargo proteins. However, how CK2 phosphorylation of acidic cluster motifs within membrane cargo and PACS-1 influence in a completely opposite manner the binding of these various acidic motifs to the PACS-1 FBR remains unknown. Moreover, acidic cluster binding to the PACS-1 FBR may be more complex than a simple phosphorylation switch, as the non-phosphorylatable Nef and PC6B acidic clusters bind to PACS-1 (Piguet *et al*., 2000; Xiang *et al*., 2000).

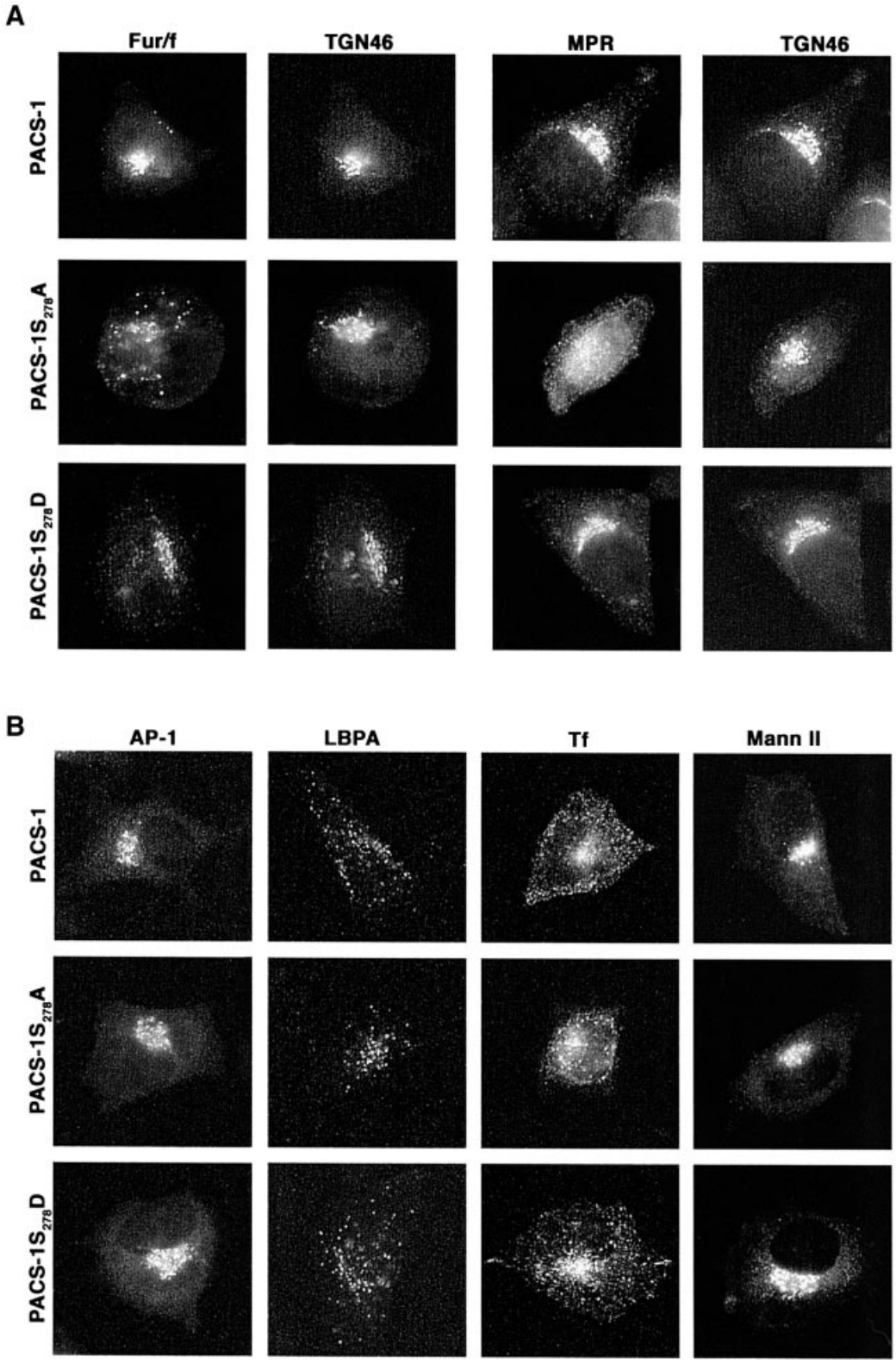

Fig. 5. Expression of PACS-1S_{278}A disrupts furin and CI-MPR localization (**A**) A7 cells were co-infected with VV co-expressing flag-tagged furin (fur/f) and PACS-1, PACS-1S_{278}A or PACS-1S_{278}D. The cells were fixed, permeabilized and incubated with anti-TGN46 and either M1 (fur/flag) or anti-CI-MPR, followed by fluorescently labeled secondary antisera. (**B**) A7 cells infected with VV expressing PACS-1, PACS-1S_{278}A or PACS-1S_{278}D were fixed, permeabilized and stained with anti-γ-adaptin, anti-LBPA and anti-mannosidase II. A replicate plate of cells was incubated with rhodamine–transferrin prior to fixation.

Blocking phosphorylation at Ser278 in PACS-1 has a profound effect on the trafficking of PACS-1 cargo. For example, the PACS-1S_{278}A mutant blocked the HIV-1 Nef-mediated downregulation of cell surface MHC-I molecules to the TGN (Figure 4) and caused the mislocalization of furin and MPR from the TGN to

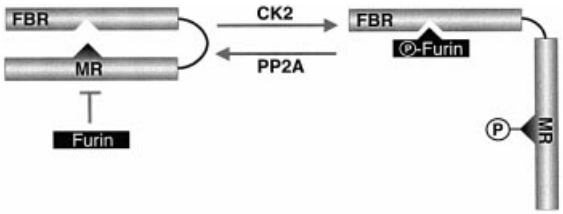

Fig. 6. A working model of the CK2/PP2A regulation of PACS-1 sorting activity. In the Ser278 non-phosphorylated state, the PACS-1 MR is bound to the PACS-1 FBR, thereby preventing cargo binding. This conformation is mimicked by PACS-1S_{278}A. CK2 phosphorylation of Ser278 disrupts the PACS-1 MR–FBR interaction and permits binding of cargo molecules to the FBR. This conformation is mimicked by PACS-1S_{278}D. In addition, CK2 phosphorylation of cargo proteins increases their affinity for activated PACS-1 and thus their association with AP-1 (Teuchert *et al*., 1999; Crump *et al*., 2001). Inactivation of PACS-1 sorting activity is achieved by PP2A-catalyzed dephosphorylation of Ser278, which promotes binding of the PACS-1 MR and FBR regions. Whether the MR and FBR domains interact intramolecularly as depicted or intermolecularly remains to be determined.

dispersed endosomal compartments (Figure 5A). The lack of a measurable effect of PACS-1S_{278}A on markers for the TGN and Golgi cisternae, as well as for early and late endosomal compartments (Figure 5B), further demonstrated the selectivity of this interfering mutant for disrupting the trafficking and localization of membrane proteins that are sorted by PACS-1. The selective disruption of protein traffic caused by PACS-1S_{278}A is very similar to that observed in cells lacking either PACS-1 (Wan *et al*., 1998) or the AP-1A adaptor (Meyer *et al*., 2000), as well as in cells expressing PACS-1Admut (Crump *et al*., 2001). Because PACS-1 forms a ternary complex with AP-1 and cargo proteins (Crump *et al*., 2001), the similar sorting defect caused by both PACS-1S_{278}A and PACS-1Admut reflects the selective inhibition of the two arms of this protein complex. Moreover, as the PACS-1S_{278}A mutation has no measurable effect on PACS-1 binding either to AP-1 (Figure 2D) or to cellular membranes (data not shown), a simple explanation for how PACS-1S_{278}A acts as an interfering mutant may be that it competes with endogenous PACS-1 for membrane recruitment and adaptor complexes but fails to bind to cargo. Alternatively, PACS-IS278A may form a non-productive complex with endogeneous PACS-1, thereby titrating out functional PACS-1.

To test directly the ability of PACS-1 to control endosome to TGN sorting, we used an *in vitro* re-sulfation assay that quantitatively measures the sorting of tyrosine-phosphorylatable reporter proteins to the TGN (Itin *et al*., 1997). We found that cytosol from control cells, but not from PACS-1 antisense cells, supports endosome to TGN transport of a tyrosine-sulfatable Nef reporter, 44Nef-Y (Figure 3). In addition, PACS-1 antisense cytosol replete with either PACS-1 or containing PACS-1S_{278}D restored endosome to TGN transport of 44Nef-Y, whereas cytosol containing PACS-1S_{278}A could not. These data combined with the immunofluorescence studies demonstrate the importance of PACS-1, and in particular the phosphorylation state of Ser278, for directing the endosome to TGN sorting of membrane cargo proteins. The requirement for PACS-1 to direct endosome to TGN transport is in agreement with earlier cell-free assays demonstrating that the phosphorylation state of the furin and CPD acidic clusters, which bind to PACS-1, have no effect on TGN budding or retention (Wan *et al*., 1998; Kalinina *et al*., 2002). Because PACS-1 is required for multiple sorting steps including endosome to TGN sorting, retrieval of furin from immature secretory granules and for recycling of phosphorylated furin from endosomes to the cell surface (Thomas, 2002), it is possible that PACS-1 participates in the retrieval of membrane proteins from multiple post-TGN compartments. The association of PACS-1 with multiple sorting adaptors (Crump *et al*., 2001; and unpublished results) further supports these multifaceted roles.

Whereas the diverse roles of autoregulatory domains in regulating processes ranging from protease activation to signal transduction are well established (Anderson *et al*., 2002; Pufall and Graves, 2002), the roles of autoregulatory domains in regulating the activities of trafficking proteins are only now beginning to emerge. Recent reports describe autoregulatory domains in the GGA1 and GGA3 adaptors, which direct anterograde sorting from the TGN to endosomes (Doray *et al*., 2002; Ghosh and Kornfeld, 2003). Similar to PACS-1, autoinhibition of GGA1 is controlled by the CK2-catalyzed phosphorylation of a serine residue (Ser355) within a cluster of acidic residues but, interestingly, in an opposite manner to that of PACS-1. Whereas CK2 phosphorylation of the PACS-1 autoregulatory domain promotes cargo binding (Figure 2), CK2 phosphorylation of the GGA1 autoregulatory domain inhibits cargo binding (Doray *et al*., 2002). Perhaps CK2 phosphorylation promotes endosome to TGN sorting by simultaneously activating PACS-1 and inhibiting GGA1. Conversely, activation of PP2A would drive movement from the TGN to endosomes by simultaneously activating GGA1 and inhibiting PACS-1. Indeed, our findings that inhibition of either CK2 or PP2A decreased or increased, respectively, the phosphorylation of endogenous PACS-1 (Figure 2) suggests that a balance in the activities of these two enzymes controls PACS-1 sorting activity. Whether GGAs and PACS-1 intimately participate in controlling protein localization is currently being investigated. Together these findings provide new insight into how the localization of membrane cargo molecules is controlled by the CK2- and PP2A-mediated activities of PACS-1 and GGAs. Elucidating the signaling pathways that control these phosphorylation events will be an important step for understanding trafficking in the TGN/endosomal system.

Materials and methods

Cell lines

BSC-40 epithelial cells, A7 melanoma cells, AS19 PACS-1 antisense cells and control C6 cells containing empty vector were cultured as previously described (Wan *et al*., 1998).

DNA constructs

pGEX3X-MR (containing PACS-1 residues 257–449) and pET32-PACS-1 FBR (containing PACS-1 residues 117–256) expressing GST and His/Trx fusion proteins were described previously (Crump *et al*., 2001). PACS-1 point mutants were generated by standard PCR methods and subcloned into pGEX3x to produce pGEX-PACS-1MRS278A, pGEX-PACS-1MRS278D and pGEX-PACS-1MRS278T. pGEX-Nef and pCMX44Nef NotI were obtained from D.Trono (Piguet *et al*., 1998, 2000). pGEX3X-CK2α was obtained from D.Litchfield.

Recombinant virus

Vaccinia virus (VV) and adenovirus (AV) were constructed using standard methods (Blagoveshchenskaya *et al*., 2002). VV recombinants expressing human hemagglutinin (HA)-tagged PACS-1 and FLAG-tagged furin were described previously (Molloy *et al*., 1994; Crump *et al*., 2001). VV recombinants expressing HA-tagged PACS-1S_{278}A and PACS-1S_{278}D were made by replacing the mutation from the pGEX-PACS-1 MR plasmid into pZVneo:PACS-1ha. The AV expressing 44Nef sequence was constructed by subcloning 44Nef from pCMX44Nef NotI into pAdtet7. 44Nef-Y was generated by inserting the cholecystokinin tyrosyl sulfation motif (SAEDYEYPS) after Lys26 of 44Nef in pAdtet44Nef.

Protein purification

pGEX or pET32a vectors encoding the various PACS-1 proteins were transformed into BL21 (DE3) or pLysS (Novagen). GST fusion proteins were purified using glutathione–agarose (Sigma) following the manufacturer's protocol. Trx fusion proteins were purified using Ni-NTA–agarose following the manufacturer's protocol (Qiagen).

Metabolic labeling and immunoprecipiations

To label recombinant PACS-1, BSC-40 cells were infected with VV expressing HA-tagged PACS-1 or PACS-1S_{278}A (m.o.i. = 10) for 4 h, washed and incubated with phosphate-free medium for 1 h. [$^{32}P_i$]Sodium orthophosphate (0.5 mCi/ml; NEN NEX053C) was then added for 3 h. The labeled cells were washed with phosphate-buffered saline (PBS), and lysed with 500 µl of mRIPA (1% NP-40, 1% sodium deoxycholate, 150 mM NaCl, 50 mM Tris pH 8.0) plus 1 mM $CaCl_2$, 50 mM NaF, 80 mM β-glycerol phosphate and 0.1 µM orthovanadate. HA-tagged PACS-1 proteins were immunoprecipitated with monoclonal antibody (mAb) HA.11 (Berkeley Antibody Co.), separated by SDS–PAGE and analyzed by autoradiography. To label endogenous PACS-1, A7 cells were grown to confluency, incubated with phosphate-free medium for 2 h, then labeled with 0.6 mCi/ml [$^{32}P_i$]sodium orthophosphate (NEN NEX053C) for 2 h in the absence or presence of either 100 µM DRB or 20 nM OA. The cells were lysed with PBS plus 1% NP-40 containing protease inhibitors (Complete, Sigma). PACS-1 was immunoprecipitated overnight using affinity-purified rabbit anti-PACS-1 antibody 601 (antigen, PACS-1 KGSLGKDTTSPME$_{433}$). The immunoprecipitates were washed, split into two, and each half separated by SDS–PAGE. One half was used for PACS-1 autoradiography and the other for control western blot with anti-PACS-1 mAb (BD Transduction Labs). Co-immunoprecipitations of PACS-1 constructs with AP-1 were performed as previously described (Crump *et al*., 2001).

In vitro phosphorylation/dephosphorylation

A 1 µg aliquot of purified GST–PACS-1 MR was incubated with 0.02 µl of purified bovine CK2 in 50 µl of reaction buffer (50 mM Tris pH 7.5, 140 mM KCl, 10 mM $MnCl_2$ and 100 µM ATP) and 10 µCi of [γ-^{32}P]ATP. The reaction mixture was incubated for 1 h at 30°C, separated by SDS–PAGE and analyzed by autoradiography. For the dephosphorylation assays, Sf9 extract containing overexpressed PP2A holoenzyme (A, C and Bα subunits) was prepared as described (Molloy *et al*., 1998). A 5 µg aliquot of CK2-phosphorylated GST–PACS-1 MR was incubated for 30 min at 37°C with 5 µl of PP2A extract and in assay buffer [25 mM Tris pH 7.4, 0.2 mM $MnCl_2$, 0.2 mg/ml bovine serum albumin (BSA) and 1 mM dithiothreitol (DTT)] in the presence or absence of 10 nM OA (Calbiochem). GST–PACS-1 MR proteins were separated by SDS–PAGE and analyzed by autoradiography.

Phosphoamino acid analysis

CK2-phosphorylated GST–MR, GST–MRs$_{278}$a and GST-MRS$_{278}$T were prepared as above except that recombinant CK2α was used. ^{32}P-Labeled proteins were separated by SDS–PAGE and either dried and exposed to X-ray film to observe protein phosphorylation or transferred to PVDF membranes. The protein bands were excised, hydrolyzed in 6 M HCl and analyzed by two-dimensional thin-layer chromatography as previously described (Jones *et al*., 1995). Radioactive samples were visualized by phosphorimage analysis.

GST protein binding assays

A 1 µg aliquot of GST, GST–MR, GST–MRS$_{278}$A, GST–MRS$_{278}$D or their CK2-phosphorylated forms was incubated with 1 µg of Trx–PACS-1 FBR in 200 µl of GST binding buffer (10 mM Tris pH 7.5, 200 mM NaCl, 1% NP-40) at room temperature for 1 h. Proteins bound to glutathione–agarose were washed with GST binding buffer and analyzed by western blot using anti-Trx mAb 46-0436 (Invitrogen). Furin competition assays were conducted as above with the addition of the indicated amounts of Trx–furin$S_{773,775}$D or Trx alone to the binding reaction for 1 h after a 1 h pre-incubation. For the GST–Nef binding experiments, A7 cells were infected with VV expressing PACS-1, PACS-1S_{278}A or PACS-1S_{278}D (m.o.i. = 5) for 16 h and lysed with GST binding buffer. A 2 µg aliquot of GST–Nef was incubated with this lysate. Bound epitope-tagged PACS-1 molecules were analyzed by western blot using the anti-HA mAb HA.11.

Immunofluorescence microscopy

Furin, MPR, TGN46, AP-1, mannosidase II, LBPA and transferrin uptake. A7 cells were grown to 80% confluency and infected with recombinant VV expressing either PACS-1, PACS-1S_{278}A or PACS-1S_{278}D alone (m.o.i. = 10), or co-infected with VV:fur/f expressing Flag-tagged furin (m.o.i. = 3) with each of the PACS-1-expressing VV recombinants (m.o.i. = 7, total m.o.i. = 10). Cells were fixed with 4% paraformaldehyde and processed for immunofluorescence as previously described (Crump *et al*., 2001; Blagoveshchenskaya *et al*., 2002). Primary antibodies to the FLAG tag (mAb M1; Kodak, 1:300), TGN46 (Serotech, 1:30), CI-MPR (from B.Hoflack, 1:200), AP-1 (mAb 100/3; Sigma, 1:50), LBPA (mAb 6C4, from J.Gruenberg, 1:10) and mannosidase II (from K.Moremen, 1:200) were used to localize antigens. Iron-loaded rhodamine–transferrin (Molecular Probes) was used as described (Crump *et al*., 2001). Following incubation with fluorescently labeled secondary antisera, all images were captured using a 63× oil immersion objective on a Leica DM-RB microscope and processed with the Scion Image 1.62 program.

MHC-I and TGN46. A7 cells grown to 80% confluency were infected with VV:WT or VV expressing HIV-1 Nef (m.o.i. = 10) or co-infected with VV expressing HIV-1 Nef (m.o.i. = 3) and either PACS-1, PACS-1S_{278}A or PACS-1S_{278}D (m.o.i. = 7, total m.o.i. = 10) for 5 h. Cells were then processed for immunofluorescence. Primary antibodies to MHC-1 (mAb w6/32; 1:100) and TGN46 (Serotech, 1:30) were incubated at 4°C overnight followed by incubation with fluorescently labeled species-specific secondary antibodies (Southern Biotech).

CD4 antibody uptake. A7 cells were infected with AV expressing 44Nef, or 44NefAla proteins for 24 h (m.o.i. = 5) then infected with VV expressing PACS-1, PACS-1S_{278}A and PACS-1S_{278}D (m.o.i. = 10) for an additional 4 h. The CD4 mAb Ab-2 (Labvision) was added to the medium for 1 h uptake and the cells were then washed and incubated in the absence of antibody for an additional 30 min. The cells were fixed with 4% paraformaldehyde, permeabilized with Triton X-100 and stained with sheep anti-TGN46 (Serotech) followed by secondary mouse–fluorescein isothiocyanate (FITC) and sheep–Texas red antibodies.

In vitro transport assay

The endosome to TGN transport assay is based on a previously published method but with several modifications (Itin *et al*., 1997).

Membrane preparation. A7 cells were cultured in sulfate-free media (Sigma) for 24 h, infected with AV expressing 44Nef-Y (m.o.i. = 2) for 16 h and then treated with 20 µg/ml cycloheximide for 4 h. The cells were washed twice with cold PBS, scraped into PBS, pelleted and resuspended in 4 ml of homogenization buffer [HB; 8.5% sucrose (w/v) in 3 mM imidazole] containing protease inhibitors (Boehringer Mannheim). The cells were passed repeatedly (~10 times) through a 22 gauge needle; post-nuclear supernatant (PNS) was collected, and sedimented over a 50% sucrose cushion (Beckman TLS 55, 45 000 r.p.m., 20 min). A 500 µl aliquot of resuspended membranes was diluted to 2 ml of H_2O, adjusted to 12.5 mM HEPES pH 7.0, 1 mM DTT, 1.5 mM MgOAc, 60 mM KCl and supplemented with 60 µl of ATP-regenerating system (100 mM ATP pH 7.0, 800 mM creatine phosphate, 4 mg/ml creatine kinase) and 10 µl of 5 mM cold PAPS, followed by incubation for 15 min at room temperature. Membranes were then diluted to 4 ml of HB, re-sedimented on a 50% sucrose cushion and stored at –70°C.

Cytosol preparation. C6 control and AS19 PACS-1 antisense cells were grown to confluency and infected with VV expressing PACS-1, PACS-1S_{278}A or PACS-1S_{278}D (m.o.i = 5) for 24 h. The cells were washed, sedimented and resuspended in 1 ml of cytosol buffer [100 mM KCl, 8.5% sucrose (w/v), 1 mM $MgCl_2$, 20 mM HEPES pH 7.4]. The resuspended cells were passed through a 22 gauge needle and the post-nuclear supernatant was clarified (Beckman TLA100.3, 45 000 r.p.m., 30 min). The cytosol layer (lower) was collected and stored at –70°C.

In vitro re-sulfation assay. A 200 μl reaction containing cytosol (1 mg/ml), donor membrane, an ATP-regenerating system and [^{35}S]PAPS (NEN, 20 μCi/assay) was incubated at 37°C for 1 h. The membranes were solubilized in IP buffer (20 mM Tris pH 7.4, 200 mM NaCl, 1% NP-40) and the 44Nef-Y- chimera was immunoprecipitated with anti-CD4 mAb Ab-4 (Calbiochem) at 4°C. Immune complexes were collected with protein G–Sepharose, separated by SDS–PAGE, analyzed by autoradiography for ^{35}S incorporation and western blotted for 44Nef-Y protein load.

Acknowledgements

We thank D.Litchfield (University of Western Ontario), J.Gruenberg (University of Geneva), B.Hoflack (Pasteur Institute), K.Moremen (University of Georgia), S.Pfeffer (Stanford University) and D.Trono (University of Geneva) for their generous gifts of reagents and advice, A.Blagoveshchenskaya (Vollum Institute) for the affinity-purified PACS-1 antiserum, D.Brickey (Vollum Institute) for help with phosphoamino acid analysis, and members of the Thomas lab for helpful discussions. This work was supported by NIH grants DK37274, AI49793 and AI48585. C.M.C. is funded by a Prize Traveling Research Fellowship from the Wellcome Trust. F.G. is funded by the Human Frontiers of Science Program.

References

Alconada,A., Bauer,U., Sodeik,B. and Hoflack,B. (1999) Intracellular traffic of herpes simplex virus glycoprotein gE: characterization of the sorting signals required for its *trans*-Golgi network localization. *J. Virol.*, **73**, 377–387.

Anderson,E.D., Molloy,S.S., Jean,F., Fei,H., Shimamura,S. and Thomas,G. (2002) The ordered and compartment-specific autoproteolytic removal of the furin intramolecular chaperone is required for enzyme activation. *J. Biol. Chem.*, **277**, 12879–12890.

Blagoveshchenskaya,A.D., Thomas,L., Feliciangeli,S.F., Hung,C.H. and Thomas,G. (2002) HIV-1 Nef downregulates MHC-I by a PACS-1- and PI3K-regulated ARF6 endocytic pathway. *Cell*, **111**, 853–866.

Bonifacino,J.S. and Traub,L.M. (2003) Signals for sorting of transmembrane proteins to endosomes and lysosomes. *Annu. Rev. Biochem.*, **72**, 395–447.

Chen,H.J., Yuan,J. and Lobel,P. (1997) Systematic mutational analysis of the cation-independent mannose 6-phosphate/insulin-like growth factor II receptor cytoplasmic domain. An acidic cluster containing a key aspartate is important for function in lysosomal enzyme sorting. *J. Biol. Chem.*, **272**, 7003–7012.

Crump,C.M., Xiang,Y., Thomas,L., Gu,F., Austin,C., Tooze,S.A. and Thomas,G. (2001) PACS-1 binding to adaptors is required for acidic cluster motif-mediated protein traffic. *EMBO J.*, **20**, 2191–2201.

Crump,C.M., Hung,C.H., Thomas,L., Wan,L. and Thomas,G. (2003) Role of PACS-1 in trafficking of human cytomegalovirus glycoprotein B and virus production. *J. Virol.*, in press.

Dittie,A.S., Thomas,L., Thomas,G. and Tooze,S.A. (1997) Interaction of furin in immature secretory granules from neuroendocrine cells with the AP-1 adaptor complex is modulated by casein kinase II phosphorylation. *EMBO J.*, **16**, 4859–4870.

Doray,B., Bruns,K., Ghosh,P. and Kornfeld,S.A. (2002) Autoinhibition of the ligand-binding site of GGA1/3 VHS domains by an internal acidic cluster–dileucine motif. *Proc. Natl Acad. Sci. USA*, **99**, 8072–8077.

Ghosh,P. and Kornfeld,S. (2003) Phosphorylation-induced conformational changes regulate GGAs 1 and 3 function at the *trans*-Golgi network. *J. Biol. Chem.*, **278**, 14543–14549.

Gruenberg,J. (2001) The endocytic pathway: a mosaic of domains. *Nature Rev. Mol. Cell Biol.*, **2**, 721–730.

Gu,F., Crump,C.M. and Thomas,G. (2001) *Trans*-Golgi network sorting. *Cell. Mol. Life Sci.*, **58**, 1067–1084.

Itin,C., Rancano,C., Nakajima,Y. and Pfeffer,S.R. (1997) A novel assay reveals a role for soluble *N*-ethylmaleimide-sensitive fusion attachment protein in mannose 6-phosphate receptor transport from endosomes to the *trans* Golgi network. *J. Biol. Chem.*, **272**, 27737–27744.

Jones,B.G., Thomas,L., Molloy,S.S., Thulin,C.D., Fry,M.D., Walsh,K.A. and Thomas,G. (1995) Intracellular trafficking of furin is modulated by the phosphorylation state of a casein kinase II site in its cytoplasmic tail. *EMBO J.*, **14**, 5869–5883.

Kalinina,E., Varlamov,O. and Fricker,L.D. (2002) Analysis of the carboxypeptidase D cytoplasmic domain: implications in intracellular trafficking. *J. Cell. Biochem.*, **85**, 101–111.

Meyer,C., Zizioli,D., Lausmann,S., Eskelinen,E.L., Hamann,J., Saftig,P., von Figura,K. and Schu,P. (2000) mu1A-adaptin-deficient mice: lethality, loss of AP-1 binding and rerouting of mannose 6-phosphate receptors. *EMBO J.*, **19**, 2193–2203.

Molloy,S.S., Thomas,L., VanSlyke,J.K., Stenberg,P.E. and Thomas,G. (1994) Intracellular trafficking and activation of the furin proprotein convertase: localization to the TGN and recycling from the cell surface. *EMBO J.*, **13**, 18–33.

Molloy,S.S., Thomas,L., Kamibayashi,C., Mumby,M.C. and Thomas,G. (1998) Regulation of endosome sorting by a specific PP2A isoform. *J. Cell Biol.*, **142**, 1399–1411.

Molloy,S.S., Anderson,E.D., Jean,F. and Thomas,G. (1999) Bi-cycling the furin pathway: from TGN localization to pathogen activation and embryogenesis. *Trends Cell Biol.*, **9**, 28–35.

Norais,N., Hall,J.A., Gross,L., Tang,D., Kaur,S., Chamberlain,S.H., Burke,R.L. and Marcus,F. (1996) Evidence for a phosphorylation site in cytomegalovirus glycoprotein gB. *J. Virol.*, **70**, 5716–5719.

Piguet,V., Chen,Y.L., Mangasarian,A., Foti,M., Carpentier,J.L. and Trono,D. (1998) Mechanism of Nef-induced CD4 endocytosis: Nef connects CD4 with the μ chain of adaptor complexes. *EMBO J.*, **17**, 2472–2481.

Piguet,V., Wan,L., Borel,C., Mangasarian,A., Demaurex,N., Thomas,G. and Trono,D. (2000) HIV-1 Nef protein binds to the cellular protein PACS-1 to downregulate class I major histocompatibility complexes. *Nature Cell Biol.*, **2**, 163–167.

Pufall,M.A. and Graves,B.J. (2002) Autoinhibitory domains: modular effectors of cellular regulation. *Annu. Rev. Cell. Dev. Biol.*, **18**

Teuchert,M., Schafer,W., Berghofer,S., Hoflack,B., Klenk,H.D. and Garten,W. (1999) Sorting of furin at the *trans*-Golgi network. Interaction of the cytoplasmic tail sorting signals with AP-1 Golgi-specific assembly proteins. *J. Biol. Chem.*, **274**, 8199–8207.

Thomas,G. (2002) Furin at the cutting edge: from protein traffic to embryogenesis and disease. *Nature Rev. Mol. Cell. Biol.*, **3**, 753–766.

Varlamov,O., Kalinina,E., Che,F.Y. and Fricker,L.D. (2001) Protein phosphatase 2A binds to the cytoplasmic tail of carboxypeptidase D and regulates post-*trans*-Golgi network trafficking. *J. Cell Sci.*, **114**, 311–322.

Waites,C.L., Mehta,A., Tan,P.K., Thomas,G., Edwards,R.H. and Krantz,D.E. (2001) An acidic motif retains vesicular monoamine transporter 2 on large dense core vesicles. *J. Cell Biol.*, **152**, 1159–1168.

Wan,L., Molloy,S.S., Thomas,L., Liu,G., Xiang,Y., Rybak,S.L. and Thomas,G. (1998) PACS-1 defines a novel gene family of cytosolic sorting proteins required for *trans*-Golgi network localization. *Cell*, **94**, 205–216.

Xiang,Y., Molloy,S.S., Thomas,L. and Thomas,G. (2000) The PC6B cytoplasmic domain contains two acidic clusters that direct sorting to distinct *trans*-Golgi network/endosomal compartments. *Mol. Biol. Cell*, **11**, 1257–1273.

Zeng,Q., Tran,T.T., Tan,H.X. and Hong,W. (2003) The cytoplasmic domain of Vamp4 and Vamp5 is responsible for their correct subcellular targeting: the N-terminal extension of VAMP4 contains a dominant autonomous targeting signal for the *trans*-Golgi network. *J. Biol. Chem.*, **278**, 23046–23054.

Received June 5, 2003; revised September 9, 2003; accepted October 8, 2003